First-Zone Distance Relaying Algorithm of Parallel Transmission Lines for Cross-Country Grounded Faults

Tianshu Bi, *Senior Member, IEEE*, Wei Li, Zhenyu Xu, *Senior Member, IEEE*, and Qixun Yang

***Abstract*—A novel distance protection algorithm for the first-zone distance relay of parallel transmission lines is proposed for cross-country grounded faults. The algorithm calculates the fault impedance using one-end sampling voltages and currents from a single line. The theoretical basis of the proposed algorithm is described in this paper, which is based on the symmetrical component method for parallel lines. And an attempt is made to express the zero-sequence current of the adjacent parallel line at the relay location by the zero-sequence current of the concerned line in combination with the fault characteristics of the system model, by which the impact of the mutual coupling between the lines can be eliminated. And, thus, the distance algorithm for cross-country grounded faults is presented. The simulations show that the proposed algorithm can obtain the accurate fault reactance when cross-country bolted faults occur, which is superior to the existing distance protection algorithm based on one-end data from a single line.**

***Index Terms*—Cross-country grounded faults, distance relaying algorithm, parallel transmission lines, symmetrical component.**

NOMENCLATURE

I, II	In subscript, they denote the variables of lines I and II for parallel lines.
A, B, and C	In subscript, they denote the electrical quantities of phases A, B, and C.
1, 2, and 0	In subscript, they denote the positive-, negative-, and zero-sequence variables.
MS, NS	In subscript, they denote the source impedances at buses M and N.
T and F	In subscript, they denote the sequence component variables of forward and reverse sequence.
K	In subscript, it denotes the fault location.
R_f and R_g	Cross-country fault resistance and the ground fault resistance, respectively.
Z_1 and X_1	They denote the total impedance and reactance of line I, respectively.
Z'_M	The line-line mutual impedance.
m, n, and p	Define the different impedance ratios between two equivalent systems.
δ	Phase angle between synchronous sources.
α	Calculating operator, which is equal to $e^{j2\pi/3}$.
D	Fractional distance from the relay location to the fault point $(0 \leq D \leq 1)$.
φ	Any phase of A, B, or C.

Manuscript received January 12, 2012; revised June 05, 2012; accepted July 16, 2012. Date of publication September 11, 2012; date of current version September 19, 2012. This work was supported in part by the National Basic Research Program (973 Program) (No. 2012CB215206), in part by the NSFC (No. 50920105705, No. 50837002), and in part by the "111 Project" (No. B08013). Paper no. TPWRD-01118-2011.

T. Bi, W. Li, and Q. Yang are with the State Key Laboratory of Alternate Electrical Power System with Renewable Energy Sources, North China Electric Power University, Beijing 102206, China.

Z. Xu is with the State Key Laboratory of Alternate Electrical Power System with Renewable Energy Sources, North China Electric Power University, Beijing 102206, China, and also with Beijing Sifang Automation Co. Ltd., Beijing 100085, China (e-mail: tsbi@ncepu.edu.cn).

Color versions of one or more of the figures in this paper are available online at http://ieeexplore.ieee.org.

Digital Object Identifier 10.1109/TPWRD.2012.2210740

I. INTRODUCTION

PARALLEL transmission lines are extensively utilized in high-voltage (HV) transmission networks [1]–[3]. Distance protection is commonly used as one of the main protections of parallel lines. However, the mutual impedance between parallel transmission lines can be as high as 50%–70% of the self-impedance for the zero-sequence coupling [4]. When conventional distance relays based on one-end sampling data from a single line are applied to parallel lines, its performance is affected by the mutual coupling between the lines, especially for cross-country faults. The protection zone of traditional distance relays without zero-sequence current compensation for parallel lines may vary from less than 50% up to far more than 100% of the total line length depending on the power system state [5].

Moreover, a failure of distance relays caused by the cross-country faults may lead to three-phase trips of both circuits. The impact of misoperations will be particularly serious under some conditions. Therefore, the protection algorithm for cross-country faults has gained an increasing interest [6].

A cross-country fault is generally caused by the fault arc from the first ground fault. There is a short time interval from the first ground fault to the cross-country fault. However, the time interval is very short compared with the fault duration time. According to the practical experience, if the time interval is within a cycle, the distance protection algorithm for the cross-country

fault has to be used instead of the traditional distance algorithm for the single-line-to-ground fault.

There are two possible solutions to consider the impact of mutual coupling between the lines. One of them is to introduce the current of the neighboring line into the distance relay of the concerned line [5]–[8]. This kind of solutions takes into account the impacts of zero-sequence mutual inductance by using sampling data from two lines, which can achieve good performance. However, bringing the neighboring line current might reduce the reliability of the relay and is not suggested in the U.K., China, and some other countries. Therefore, how to eliminate the impacts of zero-sequence mutual inductance based on one-end sampling voltages and currents from a single line is another possible solution and still an open problem.

Besides, there are two types of cross-country faults (i.e., cross-country grounded faults and cross-country ungrounded faults). For the cross-country ungrounded faults, the two zero-sequence currents of parallel lines are equal in magnitude and opposite in phase. Therefore, the fault impedance can be calculated accurately according to this characteristic [1]. When the cross-country grounded fault occurs, there is a new ground branch. The two zero-sequence currents of the parallel lines might not be equal anymore, which increases the complexity of the solution greatly.

In this paper, a novel first-zone distance-relaying algorithm is proposed for the cross-country grounded fault of parallel lines to enhance the performance of distance protection. The symmetrical component method for parallel lines is employed to decouple the mutual coupling between two lines. The zero-sequence current of the adjacent parallel line at the relay location is expressed by the zero-sequence current of the concerned line in combination with the fault characteristics of the system model. Based on this, the proposed distance-relaying algorithm is described. Simulations are made to verify the effectiveness of the algorithm by comparing the proposed algorithm with the traditional algorithms. Moreover, the factors affecting the accuracy of the proposed algorithm, such as current distribution factors, fault resistances, and line transposition condition are discussed as well.

This paper is structured as follows. Section II describes the characteristic of the zero-sequence currents. An algorithm for cross-country grounded faults is proposed in Section III. The comparisons between the proposed and the other distance relaying algorithms are shown in Section IV. Section V presents a sensitivity study including the impacts of the current distribution factors and line transposition condition. Finally, the conclusion is given in Section VI.

II. Characteristic Analysis of the Zero-Sequence Currents

The schematic diagram of parallel transmission lines for a cross-country grounded fault is shown in Fig. 1. The symmetrical component method for parallel lines is derived from the well-known symmetrical component method of a three-phase line. The sequence-component algorithm is convenient for the fault analysis of parallel lines, since it decouples the mutual induction between the parallel lines skillfully [1]. We assume that the mutual impedances between three-phase lines are the same

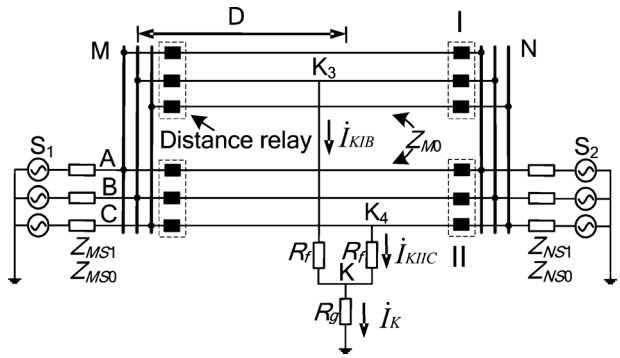

Fig. 1. System diagram of cross-country ground fault K_3 is the fault location at line I, and K_4 is the fault location at line II. The distance D from the fault locations of the two lines to the relay location M are the same.

along with the two circuits. The following analysis ignores the shunt capacitance of parallel transmission lines to simplify the algorithm.

With the symmetrical component method for parallel lines, the zero-sequence currents of parallel lines can be divided to $\dot{I}_{K0F}$ and $\dot{I}_{K0T}$ (i.e., $\dot{I}_{KI0} = \dot{I}_{K0T} + \dot{I}_{K0F}$ and $\dot{I}_{KII0} = \dot{I}_{K0T} - \dot{I}_{K0F}$). Moreover, we have (more details can be found in Appendix A)

$$\dot{I}_{K0F} = \frac{-j\sqrt{3}\dot{U}_K}{3Z_{K1T} + Z_{K1F} + 2Z_{K0F} + 6R_f} \tag{1}$$

$$\dot{I}_{K0T} = \frac{-\dot{U}_K}{Z_{K1T} + 3Z_{K1F} + 2Z_{K0T} + 6R_f + 12R_g}. \tag{2}$$

When a cross-country bolted fault occurs, R_f and R_g are both equal to 0. So (1) and (2) can be decomposed into (3) and (4), respectively

$$\dot{I}_{K0F} = -j\sqrt{3}\dot{U}_K/(3Z_{K1T} + Z_{K1F} + 2Z_{K0F}) \tag{3}$$

$$\dot{I}_{K0T} = -\dot{U}_K/(Z_{K1T} + 3Z_{K1F} + 2Z_{K0T}). \tag{4}$$

Assuming the resistances can be ignored, (5) can be obtained

$$\arg(\dot{I}_{K0F}/\dot{I}_{K0T}) = 90^\circ. \tag{5}$$

When a cross-country grounded fault with fault resistance occurs (i.e., at least one of R_f and R_g is not equal to 0), then (5) does not hold strictly. But the phase relation between I_{K0F} and I_{K0T} can be expressed as

$$\arg\left(\frac{\dot{I}_{K0F}}{\dot{I}_{K0T}}\right) = \frac{j(Z_{K1T} + 3Z_{K1F} + 2Z_{K0T} + 6R_f + 12R_g)}{3Z_{K1T} + Z_{K1F} + 2Z_{K0F} + 6R_f}. \tag{6}$$

A qualitative conclusion can be derived by analyzing the extreme conditions of R_f and R_g. When R_f and R_g approach 0, the angle $\arg(\dot{I}_{K0F}/\dot{I}_{K0T})$ approximates to 90°. When R_f approaches infinity and R_g approaches 0, the angle approximates to 90°. When R_f approaches 0 and R_g approaches infinity, the angle approximates to 0. So the variable range of the angle is 0 to 90°. According to the phase relation between $\dot{I}_{K0F}$ and

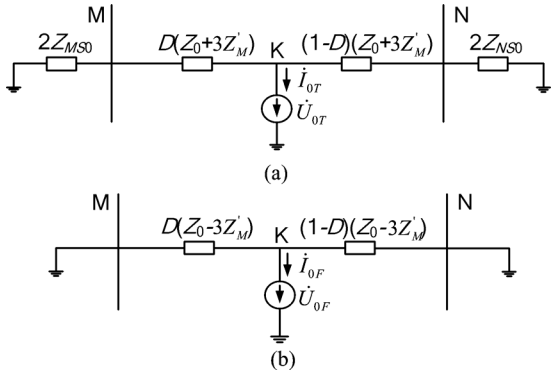

Fig. 2. Zero-sequence distribution networks of the fault component. (a) Forward-component distribution network of zero sequence. (b) Reverse-component distribution network of zero sequence.

$\dot{I}_{K0T}$, the phase relation between the zero-sequence currents of parallel lines can be obtained, which will be used for the derivation of the distance algorithm.

III. Algorithm for First-Zone Distance Relay

When a cross-country grounded fault (IBIICG) occurs, applying Kirchhoff's Voltage Law (KVL) for the circuit from the relay location M to the fault location K in Fig. 1, gives (7), shown at the bottom of the page. More explicitly, $K_0 = (Z_0 - Z_1)/Z_1$, $K_{M0} = Z_{M0}/Z_1$.

Supposing that the fault is the cross-country bolted fault, R_f and R_g are both equal to 0. Then, we have

$$\begin{cases} \dot{I}_{MI0} = 3C_{M0T}\dot{I}_{K0T} + 3C_{M0F}\dot{I}_{K0F} \\ \dot{I}_{MII0} = 3C_{M0T}\dot{I}_{K0T} - 3C_{M0F}\dot{I}_{K0F} \end{cases} \tag{8}$$

where C_{M0T} and C_{M0F} are the forward- and reverse-component distribution factors of the zero-sequence current at the relay location M, respectively.

Fig. 2 gives the schematic diagram for the zero-sequence distribution networks of the fault component. The distribution factors of the forward- and reverse-zero-sequence currents are formulated as follows [1]:

$$\begin{cases} C_{M0T} = \dfrac{(1-D)(Z_0+3Z_{M0})+2Z_{NS0}}{2Z_{MS0}+Z_0+3Z_{M0}+2Z_{NS0}} \\ C_{M0F} = 1-D \end{cases}. \tag{9}$$

The system components are assumed as the inductive reactance components, so the distribution factors C_{M0T} and C_{M0F} are both real numbers. Suppose the angle β is the phase difference between $\dot{I}_{MI0}$ and $\dot{I}_{MII0}$. According to (5) and (8), the relation between $\dot{I}_{MI0}$ and $\dot{I}_{MII0}$ is expressed as

$$\dot{I}_{MII0} = \dot{I}_{MI0}\angle\beta. \tag{10}$$

Substituting (10) into (7)

$$\dot{U}_{MIB} = DZ_1(\dot{I}_{MIB} + K_0\dot{I}_{MI0} + K_{M0}\dot{I}_{MI0}\angle\beta). \tag{11}$$

The fault distance D is obtained as follows:

$$D = \frac{\dot{U}_{MIB}}{Z_1(\dot{I}_{MIB} + K_0\dot{I}_{MI0} + K_{M0}\dot{I}_{MI0}\angle\beta)}. \tag{12}$$

It follows from (8) and (10) that

$$\angle\beta = \frac{\dot{I}_{MII0}}{\dot{I}_{MI0}} = \frac{3C_{M0T}\dot{I}_{K0T} - 3C_{M0F}\dot{I}_{K0F}}{3C_{M0T}\dot{I}_{K0T} + 3C_{M0F}\dot{I}_{K0F}}. \tag{13}$$

According to (11), the angle β is expressed by eliminating the fault distance D from the real and imaginary parts as

$$\frac{a_1}{b_1} = \frac{a_2 + a_3\cos(\beta+\theta)}{b_2 + b_3\sin(\beta+\theta)}. \tag{14}$$

More explicitly

$$\begin{aligned} a_1 &= \mathrm{real}(\dot{U}_{MIB}/Z_1), \\ b_1 &= \mathrm{imag}(\dot{U}_{MIB}/Z_1). \\ a_2 &= \mathrm{real}(\dot{I}_{MIB} + K_0\dot{I}_{MI0}), \\ b_2 &= \mathrm{imag}(\dot{I}_{MIB} + K_0\dot{I}_{MI0}). \\ a_3 &= b_3 = K_{M0}I_{MI0}. \end{aligned}$$

Then, (14) can be changed as

$$a_3b_1\cos(\beta+\theta) - a_1b_3\sin(\beta+\theta) = a_1b_2 - a_2b_1. \tag{15}$$

Then, (15) can be written as

$$\sin(r_1 - (\beta+\theta)) = \sin r_2. \tag{16}$$

More explicitly

$$\begin{cases} \sin r_1 = a_3b_1/\sqrt{(a_3b_1)^2 + (a_1b_3)^2} \\ \cos r_1 = a_1b_3/\sqrt{(a_3b_1)^2 + (a_1b_3)^2} \end{cases}. \\ \sin r_2 = (a_1b_2 - a_2b_1)/\sqrt{(a_3b_1)^2 + (a_1b_3)^2}.$$

The following is the basic rule of the trigonometric function:

$$\sin(180^\circ - r_2) = \sin r_2. \tag{17}$$

According to (16) and (17), the two results of β are derived

$$\begin{cases} \beta_1 = r_1 - (180^\circ - r_2) - \theta \\ \beta_2 = r_1 - r_2 - \theta \end{cases}. \tag{18}$$

To obtain the variation range of angle β, several assumptions are considered. For a given line, the line parameters may be considered as constants, which are shown in Appendix B. The range of angle β should be determined by (13) for various fault locations and possible system configurations. An example of this is shown in Fig. 3. It is evident that β belongs to -90° to

$$\begin{cases} \dot{U}_{MIB} - \dot{U}_{K3IB} = DZ_1(\dot{I}_{MIB} + K_0\dot{I}_{MI0} + K_{M0}\dot{I}_{MII0}) \\ \dot{U}_{MIIC} - \dot{U}_{K4IIC} = DZ_1(\dot{I}_{MIIC} + K_0\dot{I}_{MII0} + K_{M0}\dot{I}_{MI0}) \\ \dot{U}_{K3IB} - \dot{I}_{KIB}R_f = \dot{U}_{K4IIC} - \dot{I}_{KIIC}R_f = \dot{I}_K R_g \end{cases}. \tag{7}$$

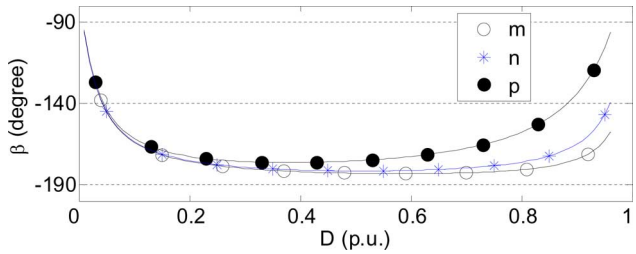

Fig. 3. Variation of angle β as a function of fault location for different source impedance ratios. $Z_{MS1} = \mathrm{j}6.0\ \Omega$, $Z_{MS0} = \mathrm{j}7.8\ \Omega$, $\mathrm{m} \div (Z_{MS1}/Z_{NS1}) = 0.1$, $\mathrm{n} \div (Z_{MS1}/Z_{NS1}) = 1$, and $\mathrm{p} \div (Z_{MS1}/Z_{NS1}) = 10$.

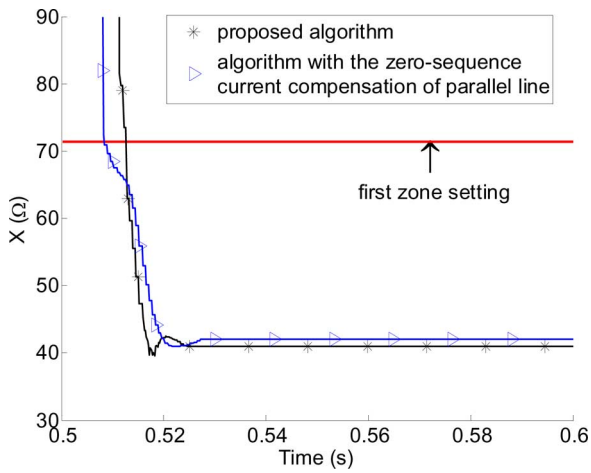

Fig. 4. Estimated fault reactance under the IBIICG bolted fault with a fault location of 150 km from bus M.

-180°. According to this conclusion that β belongs to -90° to -180°, β_1 meets the requirement.

On the basis of the conclusion derived before, the angle β in (12) can be determined

$$\beta = r_1 - (180^\circ - r_2) - \theta. \tag{19}$$

More explicitly

$$r_1 = \arcsin(a_3 b_1 / \sqrt{(a_3 b_1)^2 + (a_1 b_3)^2}).$$
$$r_2 = \arcsin((a_1 b_2 - a_2 b_1) / \sqrt{(a_3 b_1)^2 + (a_1 b_3)^2}).$$

Note that D represents the distance, which can make up a distance relay. Substituting (19) into (12), the estimated inductive reactance at the relay location is obtained

$$X = DX_1. \tag{20}$$

Similarly, performance equations for the estimated inductive reactance for other types of cross-country faults can be derived. In the derived formula (12), $\dot{U}_{MIB}, \dot{I}_{MIB}$ should be replaced by the fault-phase voltage and fault-phase current, respectively.

IV. Case Studies

The simulation model of a 500-kV equivalent two-machine system is shown in Fig. 1, and the detailed parameters are presented in Appendix B. The PSCAD/EMTDC simulation software is employed for power system simulation. Source M leads source N by 30° (heavy load) and 0° (no load). Faults are initiated at 0.5 s. The full-cycle Fourier correlation has been applied as a filter algorithm using a sampling rate of 100 samples/cycle (for a 50-Hz system). Only the fundamental frequency component is evaluated. Equation (20) is employed to calculate the estimated fault reactance from the relay location to the fault location.

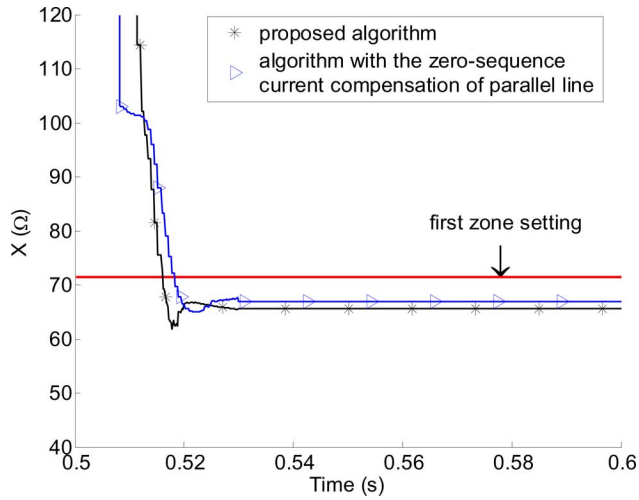

Fig. 5. Estimated fault reactance under the IBIICG bolted fault with a fault location of 240 km from bus M.

In order to evaluate the proposed algorithm, some comparison results are shown between the proposed algorithm, and the algorithm with direct zero-sequence current compensation of the parallel lines or the traditional algorithm without zero-sequence current compensation of the parallel lines.

The algorithm with direct zero-sequence current compensation of the parallel lines is given

$$X = \mathrm{imag}(\dot{U}_{MI\phi} / (\dot{I}_{MI\phi} + K_0 \dot{I}_{MI0} + K_{M0} \dot{I}_{MII0})). \tag{21}$$

The traditional algorithm without the zero-sequence current compensation of the parallel lines can be expressed as

$$X = \mathrm{imag}(\dot{U}_{MI\phi} / (\dot{I}_{MI\phi} + K_0 \dot{I}_{MI0})). \tag{22}$$

Figs. 4 and 5 show the comparison results between the proposed algorithm and the algorithm with the zero-sequence current compensation of the parallel lines when IBIICG bolted faults occur in two different locations. Once the fault phase is selected, the proposed algorithm can calculate the fault reactance within a cycle (20 ms). It can be seen that the first few estimates are erroneous because the data window mainly contains prefault data. When the data window is filled with postfault data, the estimates approach the actual fault reactance gradually.

The zero-sequence current of parallel transmission lines is used to compensate the mutual coupling effect in inductive reactance measurement on the faulted line in (21). The distance measurement with fully compensated zero-sequence current of the parallel transmission lines on fault lines will always be correct when both lines of the parallel lines are in operation [8]. Therefore, the algorithm with the zero-sequence current compensation of the parallel lines can obtain an accurate fault reactance. As shown in Figs. 4 and 5, the loci of the proposed algorithm approach the loci of the algorithm with the zero-sequence

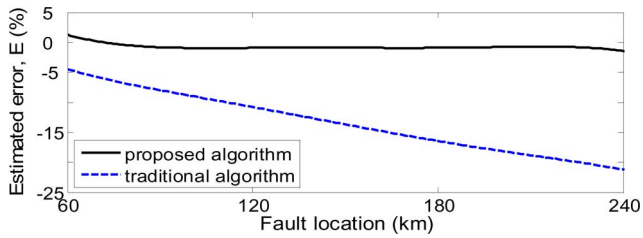

Fig. 6. Estimated fault reactance errors under the IBIICG bolted fault with the condition of $\delta = 30°$ under different fault locations.

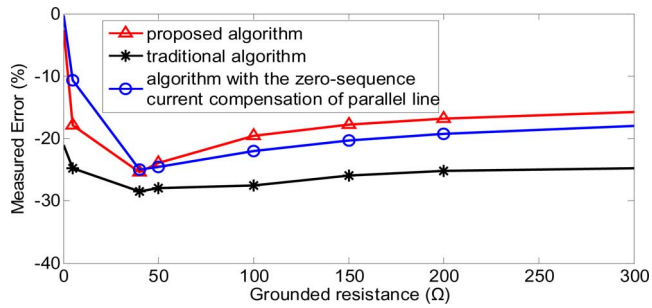

Fig. 7. Estimated fault reactance errors under the IBIICG resistance grounded fault with the condition of R_f equal to 0 and R_g within 0–300 Ω with a fault location of 240 km from bus M.

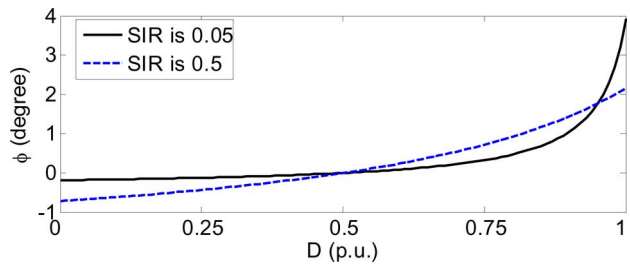

Fig. 8. Variation of ϕ as a function of fault location for two different source-to-line impedance ratios $Z_{MS0} = Z_{NS0}$.

current compensation of the parallel lines in different fault locations. The results indicate that the performance of the proposed algorithm is close to the algorithm with the zero-sequence current compensation of the parallel lines.

The maximum error of the proposed algorithm is less than 3% in Fig. 5. The errors exist due to the assumed condition that the system is not completely composed of the strictly inductive components and the source impedances have an insignificant impact on the distribution factors, but the maximal value is less than 3% that should be acceptable. The simulation in Fig. 5 shows that both of the aforementioned algorithms can operate correctly when a normal 85% zone coverage for zone one is set. Therefore, the proposed algorithm can satisfy the accuracy requirements of the first-zone distance relay under the cross-country bolted faults.

The zero-sequence current of the parallel transmission lines is not always available for the relay in practice in some cases. The traditional algorithm without zero-sequence current compensation of the parallel lines may either overreach or underreach, depending upon the relative direction of the parallel transmission lines' zero-sequence current. To verify the proposed algorithm, the comparisons between the proposed algorithm and the traditional algorithm without the zero-sequence current compensation of the parallel lines are given in two typical conditions.

Fig. 6 shows the comparisons between the proposed algorithm and the traditional algorithm without the zero-sequence current compensation of the parallel lines when IBIICG bolted faults occur. The faults are simulated with $\delta = 30°$ (heavy load, source M leads source N) under different fault locations. As shown in Fig. 6, the estimated errors of the proposed algorithm are much smaller than those of the traditional algorithm. The relay with the proposed algorithm can operate correctly under this condition when the relay with the traditional algorithm may overreach.

The fault resistance between the fault phases is small in practice, but the ground resistance might be large [9]. A simulation is given under the extreme conditions of $\delta = 30°$ and R_f equal to 0 Ω and R_g within 0–300 Ω. The estimated errors of three algorithms are shown in Fig. 7. The error of the estimated fault reactance is calculated

$$E = (X - X_a)/X_1 \tag{23}$$

where X_a is the actual fault reactance of line I.

According to Fig. 7, it can be seen that the estimated error of the proposed algorithm is quite small when the ground resistance is small, which is superior to the traditional algorithm. Therefore, the application of the proposed algorithm can enhance the performance of the distance protection on parallel lines.

V. Sensitivity Studies

In the derived formula from before, it is assumed that two lines are fully transposed, and a cross-country grounded fault occurs. However, in practice, the case may not be ideal. Therefore, it is necessary to analyze the sensitivity of the proposed algorithm to the error of the parameters.

A. Impact of Current Distribution Factors

The proposed algorithm for distance relaying needs the current distribution factor C_{M0T} in (9) to be a real number. An exact real number will not be always accessible, for it depends upon the system and transmission-line parameters. When the fault location changes along the parallel transmission lines, the phase angle ϕ of the current distribution factor varies in a certain range. The variation of the angle ϕ along the different fault location is shown in Fig. 8.

Fig. 8 shows the variation of the angle ϕ against the fault location for two extreme source-to-line impedance ratios (SIRs). As shown in Fig. 8, the maximum value of the phase angle ϕ is only 3.92 (solid line) when the fault is near the end of the transmission line. The value lead to a maximum estimated error approaching -2% (corresponding to the point at the end of the solid line of Fig. 6). Therefore, the variation of the phase angle of C_{M0T} is very small in Fig. 8, resulting in a negligible impact on the estimated fault reactance, as shown in the solid line of Fig. 6.

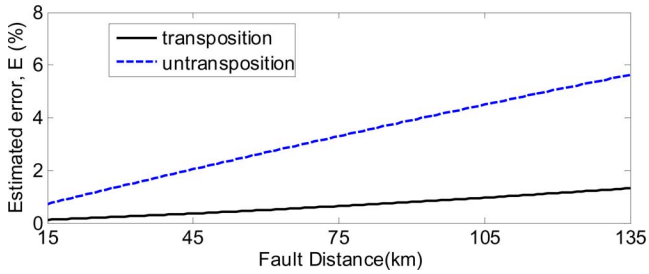

Fig. 9. Estimated fault reactance error by applying the proposed algorithm for transposition and nontransposition lines.

B. Impact of Fault Resistances

It can be concluded that the proposed algorithm is associated with the fault resistance from the derived formulas (1) and (2). Figs. 4 and 5 show that the proposed algorithm has good performance when a cross-country bolted fault occurs. As shown in Figs. 6 and 7, the proposed algorithm has better performance than the traditional algorithm without the zero-sequence current compensation of the parallel lines for the cross-country grounded fault with high fault resistances.

C. Impact of the Line Transposition Condition

It has been assumed that the parallel transmission lines are perfectly transposed and three phases of two lines are symmetrical in the previous analysis. If the lines are not perfectly transposed, the sequence impedances depend upon the line geometry. If the untransposed line parameters are used to substitute for the transposed line parameters, it will bring some errors to the proposed algorithm.

The configuration of the tower structure for 500-kV transmission lines is presented in Fig. 12, and the length of the line is 150 km. For a first-zone distance relay whose setting range reaches 80%–90% of the protected line, it is often expected that the error will be less than ±5% around the reach of the setting [10]. Fig. 9 shows that the estimated fault resistance error is less than 5% when the fault location is close to the end of the first-zone setting (127.5 km). Therefore, the error has a negligible effect on the application of the proposed algorithm to first-zone protection for the untransposed line.

VI. Conclusion

The performance of conventional distance relays on parallel lines is adversely affected by the mutual coupling effect between the lines, especially for cross-country faults. The traditional distance relay without the zero-sequence current compensation for parallel transmission lines may overreach. A novel algorithm of first-zone distance relaying is proposed for cross-country grounded faults in this paper. The zero-sequence current of the adjacent parallel lines at the relay location is expressed by the zero-sequence current of the concerned line using the symmetrical component method for parallel lines. The accuracy of the proposed algorithm is analyzed under all kinds of fault conditions. The simulation results demonstrate that the proposed algorithm is as good as the algorithm with direct zero-sequence current compensation of the parallel lines; while it achieves better performance compared with the traditional algorithm without zero-sequence current compensation of the parallel lines.

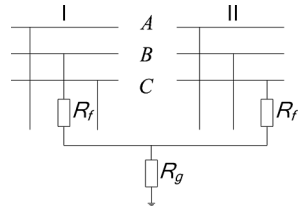

Fig. 10. Fault boundary condition of IBIICG.

Appendix A

The coupled transmission equations are transformed into decoupled ones depending on the sequence-component algorithm of parallel lines. More details can be found in [1].

An example of an analysis IBIICG fault based on the sequence-component algorithm is given here. In case of cross-country grounded faults, the fault boundary condition of IBIICG is shown in Fig. 10.

The cross-country fault resistance R_f is added to the system impedances, this strategy is similar to the management of the phase-phase fault resistance of a single line using the symmetrical component method. Therefore, the sequence components of voltage would be added to the superscript "′" in the next formula for distinction. Z_{K0T} can be replaced by Z'_{K0T}, and so can the other sequence components.

More explicitly, $Z'_{K0T} = Z_{K0T} + R_f, Z'_{K0F} = Z_{K0F} + R_f$

$$Z'_{K1T} = Z_{K1T} + R_f, \quad Z'_{K1F} = Z_{K1F} + R_f,$$
$$Z'_{K2T} = Z_{K2T} + R_f, \quad Z'_{K2F} = Z_{K2F} + R_f.$$

For the fault boundary condition shown in Fig. 10, the following equations are obtained by applying the KVL and KCL at the fault location K:

$$\begin{cases} \dot{U}_{KIB} = \dot{U}_{KIIC} \\ \dot{I}_{KIB} + \dot{I}_{KIIC} = \dot{I}_K \\ \dot{I}_{KIA} = \dot{I}_{KIIA} = \dot{I}_{KIC} = \dot{I}_{KIIB} = 0. \end{cases} \tag{A1}$$

The mutual coupling between two lines can be decoupled by sequence components, which are nominated T component and F component. As shown in Fig. 11, it can be seen that the T component has equal quantities in both lines; the F component has antiequal quantities in both lines (equal in magnitude but opposite in sign). Therefore, the T component and F component are also called the forward component and reverse component, respectively. Then, (A1) can be written as

$$\begin{cases} \dot{U}_{\mathrm{KTB}} + \dot{U}_{\mathrm{KFB}} = \dot{U}_{\mathrm{KTC}} - \dot{U}_{\mathrm{KFC}} \\ \dot{I}_{\mathrm{KTB}} + \dot{I}_{\mathrm{KFB}} + \dot{I}_{\mathrm{KTC}} - \dot{I}_{\mathrm{KFC}} = \dot{I}_K \\ \dot{I}_{\mathrm{KTA}} = \dot{I}_{\mathrm{KFA}} = 0 \\ \dot{I}_{\mathrm{KTC}} + \dot{I}_{\mathrm{KFC}} = 0 \\ \dot{I}_{\mathrm{KTB}} - \dot{I}_{\mathrm{KFB}} = 0. \end{cases} \tag{A2}$$

Due to the sequence-component algorithm, the following equations are obtained from (A2).

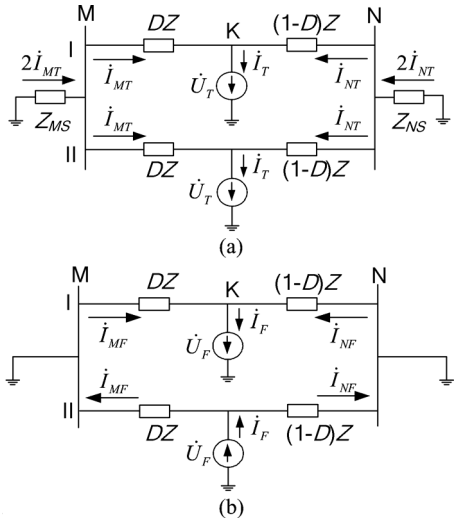

Fig. 11. Sequence distribution networks of T and F components. (a) The T component distribution network of the fault component. (b) The F component distribution network of the fault component.

The next results are derived from (A3), shown at the bottom of the page.

Applying the KCL at the fault location

$$\dot{I}_K = (\alpha^2+\alpha)\dot{I}_{K1T} + (\alpha^2-\alpha)\dot{I}_{K1F} + (\alpha^2+\alpha)\dot{I}_{K2T} + (\alpha-\alpha^2)\dot{I}_{K2F} + 2\dot{I}_{K0T}. \quad \text{(A5)}$$

Substituting (A4), shown at the bottom of the page, into (A5)

$$\dot{I}_K = 6\dot{I}_{K0T}. \quad \text{(A6)}$$

Due to the sequence-component algorithm, the following equations are obtained by applying the KVL at the fault location:

$$\dot{U}'_{KIB} = \alpha^2(\dot{U}_K - Z'_{K1T}\dot{I}_{K1T} - Z'_{K1F}\dot{I}_{K1F}) - \alpha(Z'_{K1T}\dot{I}_{K2T} + Z'_{K1F}\dot{I}_{K2F}) - Z'_{K0T}\dot{I}_{K0T} - Z'_{K0F}\dot{I}_{K0F} \quad \text{(A7)}$$

$$\dot{U}'_{KIIC} = \alpha(\dot{U}_K - Z'_{K1T}\dot{I}_{K1T} + Z'_{K1F}\dot{I}_{K1F}) - \alpha^2(Z'_{K1T}\dot{I}_{K2T} - Z'_{K1F}\dot{I}_{K2F}) - Z'_{K0T}\dot{I}_{K0T} + Z'_{K0F}\dot{I}_{K0F} \quad \text{(A8)}$$

$$\dot{U}'_{KIB} = \dot{U}'_{KIIC}. \quad \text{(A9)}$$

Substituting (A7) and (A8), into (A9)

$$\dot{I}_{K0F} = -j\sqrt{3}\dot{U}_K/(3Z'_{K1T} + Z'_{K1F} + 2Z'_{K0F}) \quad \text{(A10)}$$

$$\dot{I}_{K0F} = -j\sqrt{3}\dot{U}_K/(3Z_{K1T} + Z_{K1F} + 2Z_{K0F} + 6R_f). \quad \text{(A11)}$$

When R_f is added to the system impedances, both K_3 and K_4 coincide with K. The following equation is derived by applying Ohm's Law at the fault location

$$\dot{U}'_{KIB} = \dot{U}'_{KIIC} = \dot{U}_K = \dot{I}_K R_g. \quad \text{(A12)}$$

Substituting (A8) and (A9), into (A12)

$$\dot{I}_{K0T} = -\dot{U}_K/(Z'_{K1T} + 3Z'_{K1F} + 2Z'_{K0T} + 12R_g) \quad \text{(A13)}$$

$$\dot{I}_{K0T} = -\dot{U}_K/(Z_{K1T} + 3Z_{K1F} + 2Z_{K0T} + 6R_f + 12R_g). \quad \text{(A14)}$$

Appendix B
Parameters of the 300-km, 500-kV Bergeron Model Lines

Positive-/negative-sequence parameters:
- $R = 0.022\ \Omega$/km;
- $X_L = 0.28\ \Omega$/km;
- $X_C = 0.24114\ \mathrm{M}\Omega$-km.

Zero-sequence parameters:
- $R_0 = 0.182\ 8\ \Omega$/km;
- $X_{L0} = 0.86\ \Omega$/km;
- $X_{C0} = 0.57875\ \mathrm{M}\Omega$-km;
- $Z_{M0} = 0.522\ \Omega$/km.

S1 parameters:
- $X_{MS1} = X_{MS2}$: 6.0 Ω(min), 67.0 Ω(max);
- X_{MS0}: 7.8 Ω(min), 78.0 Ω(max).

S2 parameters:
- $X_{NS1} = X_{NS2}$: 9.0 Ω(min), 182.0 Ω(max);
- X_{NS0}: 18.2 Ω(min), 364.0 Ω(max).

$$\begin{cases} \alpha^2\dot{U}'_{K1T} + \alpha\dot{U}'_{K2T} + \dot{U}'_{K0T} + \alpha^2\dot{U}'_{K1F} + \alpha\dot{U}'_{K2F} + \dot{U}'_{K0F} \\ \quad = \alpha\dot{U}'_{K1T} + \alpha^2\dot{U}'_{K2T} + \dot{U}'_{K0T} - (\alpha\dot{U}'_{K1F} + \alpha^2\dot{U}'_{K2F} + \dot{U}'_{K0F}) \\ \alpha^2\dot{I}_{K1T} + \alpha\dot{I}_{K2T} + \dot{I}_{K0T} + \alpha^2\dot{I}_{K1F} + \alpha\dot{I}_{K2F} + \dot{I}_{K0F} + \alpha\dot{I}_{K1T} \\ \quad + \alpha^2\dot{I}_{K2T} + \dot{I}_{K0T} - (\alpha\dot{I}_{K1F} + \alpha^2\dot{I}_{K2F} + \dot{I}_{K0F}) = \dot{I}_K \\ \dot{I}_{K1T} + \dot{I}_{K2T} + \dot{I}_{K0T} = 0 \\ \dot{I}_{K1F} + \dot{I}_{K2F} + \dot{I}_{K0F} = 0 \\ \alpha\dot{I}_{K1T} + \alpha^2\dot{I}_{K2T} + \dot{I}_{K0T} = -(\alpha\dot{I}_{K1F} + \alpha^2\dot{I}_{K2F} + \dot{I}_{K0F}) \\ \alpha^2\dot{I}_{K1T} + \alpha\dot{I}_{K2T} + \dot{I}_{K0T} = \alpha^2\dot{I}_{K1F} + \alpha\dot{I}_{K2F} + \dot{I}_{K0F} \end{cases}. \quad \text{(A3)}$$

$$\begin{cases} \dot{I}_{K1T} = \dfrac{j\sqrt{3}}{2}\dot{I}_{K0F} - \dfrac{1}{2}\dot{I}_{K0T}, \dot{I}_{K2T} = \dfrac{-j\sqrt{3}}{2}\dot{I}_{K0F} - \dfrac{1}{2}\dot{I}_{K0T} \\ \dot{I}_{K1F} = \dfrac{j\sqrt{3}}{2}\dot{I}_{K0T} - \dfrac{1}{2}\dot{I}_{K0F}, \dot{I}_{K2F} = \dfrac{-j\sqrt{3}}{2}\dot{I}_{K0T} - \dfrac{1}{2}\dot{I}_{K0F} \end{cases}. \quad \text{(A4)}$$

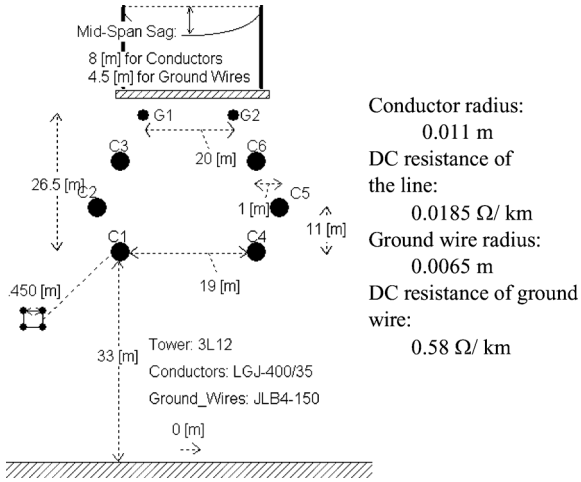

Fig. 12. Configuration of the tower structure.

For parameters of the 150-km, 500-kV asymmetrical and untransposed lines, see Fig. 12.

ACKNOWLEDGMENT

The authors would like to thank Profs. A. G. Phadke and J. S. Thorp for their comments on this paper when they worked in Beijing on the "111" Project.

REFERENCES

[1] Z. Y. Xu, W. Li, T. S. Bi, G. Xu, and Q. X. Yang, "First-zone distance relaying algorithm of parallel transmission lines for cross-country non-earthed faults," *IEEE Trans. Power Del.*, vol. 26, no. 4, pp. 2486–2494, Oct. 2011.

[2] M. I. Gilany, O. P. Malik, and G. S. Hope, "A digital technique for parallel transmission lines using a single relay at each end," *IEEE Trans. Power Del.*, vol. 7, no. 1, pp. 118–123, Jan. 1992.

[3] Y. Liao and S. Elangovan, "Digital distance relaying algorithm for first-zone protection for parallel transmission lines," in *Proc. Inst. Elect. Eng., Gen. Transm. Distrib.*, Sep. 1998, vol. 145, no. 5, pp. 531–536.

[4] B. R. Bhalja and R. P. Maheshwari, "High-resistance faults on two terminal parallel transmission line: Analysis, simulation studies, and an adaptive distance relaying scheme," *IEEE Trans. Power Del.*, vol. 22, no. 2, pp. 801–812, Apr. 2007.

[5] A. G. Jongepier and L. van der Sluis, "Adaptive distance protection of a double circuit line," *IEEE Trans. Power Del.*, vol. 9, no. 3, pp. 1289–1297, Jul. 1994.

[6] A. G. Phadke and J. H. Lu, "A new computer based integrated distance relay for parallel transmission lines," *IEEE Trans. Power App. Syst.*, vol. PAS-104, no. 2, pp. 445–452, Feb. 1985.

[7] P. G. McLaren, I. Fernando, H. Liu, E. Dirks, G. W. Swift, and C. Steele, "Enhanced double circuit line protection," *IEEE Trans. Power Del.*, vol. 12, no. 3, pp. 1100–1108, Jul. 1997.

[8] H. Yi, D. Novosel, M. M. Saha, and V. Leitloff, "An adaptive scheme for parallel-line distance protection," *IEEE Trans. Power Del.*, vol. 17, no. 1, pp. 105–110, Jan. 2002.

[9] A. Wiszniewski, "Accurate fault impedance locating algorithm," *Proc. Inst. Electy. Eng. Proceedings*, vol. 130, no. 6, pp. 311–314, Nov. 1983.

[10] Z. Y. Xu, S. F. Huang, L. Ran, J. F. Liu, Q. X. Yang, and J. L. He, "A distance relay for a 1000-kV UHV transmission line," *IEEE Trans. Power Del.*, vol. 23, no. 4, pp. 1795–1804, Oct. 2008.

Tianshu Bi (M'98–SM'09) received the Ph.D. degree in electrical and electronics engineering at the University of Hong Kong, Hong Kong, China, in 2002.

Currently, she is a Professor with North China Electric Power University, Beijing, China. Her research interests include power system protection and control, synchronized phasor-measurement techniques, as well as application and fault diagnosis.

Wei Li was born in China in 1983. He is currently pursuing the Ph.D. degree in electrical engineering at North China Electric Power University, Beijing, China.

His research interests include power system protection and control.

Zhenyu Xu (M'08-SM'10) was born in 1963. He received the Ph.D. degree in electrical engineering from North China Electric Power University, Beijing, China.

Currently, he is a Professor at North China Electric Power University. While with Sifang Automation Co. Ltd., he designed a series of ultra-high-voltage/extremely high-voltage transmission-line protection relays, which have been widely used on 220–1000-kV transmission lines in China. His research interests include power system protection and control.

Qixun Yang was born in China in 1937.

Currently, he is a Chinese Academician of Engineering and a Professor at North China Electric Power University, Beijing, China. His research interests include power system protection and control, and substation automation.